

Supporting Information

Chlorine Isotope Fractionation of the Major Chloromethane Degradation Processes in the Environment

Frank Keppler,^{,†} Jaime D. Barnes,[#] Axel Horst,[§] Enno Bahlmann,[‡] Jing Luo,^{||} Thierry Nadalig,^{||} Markus Greule,[†] S. Christoph Hartmann,^{†,⊥} and Stéphane Vuilleumier^{||}*

[†]Institute of Earth Sciences, Heidelberg University, Im Neuenheimer Feld 236, Heidelberg, Germany

[#]Department of Geological Sciences, University of Texas, Austin, TX 78712, United States

[§]Department of Isotope Biogeochemistry, Helmholtz Centre for Environmental Research – UFZ, Permoserstr.15, 04318 Leipzig, Germany

[‡]Leibniz Institute for Baltic Sea Research Warnemünde, Seestrasse 15, 18119 Rostock, Germany

^{||}Université de Strasbourg UMR 7156 CNRS, Génétique Moléculaire, Génomique, Microbiologie, 4 allée Konrad Roentgen, 67000 Strasbourg, France

[⊥]Max Planck Institute for Chemistry, Hahn-Meitner-Weg 1, 55128 Mainz, Germany.

*Corresponding author's email: frank.keppler@geow.uni-heidelberg.de

Content:

Table: S1

Methods: S1-S3

Figures: S1-S9

References

11 Pages

Sample preparation

Table S1: Smog chamber experiments with CH₃Cl. Summary of the experimental details for the degradation of CH₃Cl with ·OH and ·Cl radicals performed in 3,500 L Teflon smog-chamber. Technical details of the design of the smog chamber and performed degradation experiments were previously reported^{1, 2}.

reaction	Initial CH ₃ Cl		Oxidant				
	mixing ratio	Irradiation	O ₃ /Cl ₂ mixing ratio	Rel. hum.	H ₂ initial	T	OH
	ppmv		ppmv	%	ppmv	°C	cm ⁻³
CH ₃ Cl + OH ^a	10	1x55W, λ _{max} = 254 nm	0.62	65	2000	20.7	2.9 x 10 ⁹
CH ₃ Cl + Cl ^b	10	7x1200W, 300 - 700 nm	2 to 10	< 1		20.7	

^a Same experiment as described in Bahlmann et al.¹ and Keppler et al.²

^b Same experiment as described in Bahlmann et al.¹

Method S1: Stable chlorine isotope analyses using GC-MS

In addition to GC-MC-ICPMS measurements, GC-MS data from concentration measurements were used to derive chlorine isotope fractionation for CH₃Cl degradation by ·OH and ·Cl radicals in smog chamber experiments (Figs. S1 and S2). Briefly, the GC-MS used to monitor mixing ratios in the smog chamber experiments (see Table S1) was operated in electron impact selective ion recording mode with a mass resolution of 0.5 amu. Chlorine isotope ratios were calculated from the abundances of CH₃³⁵Cl⁺ (m/z 50) and CH₃³⁷Cl⁺ (m/z 52) ions respectively, and expressed as delta values in ‰ relative to the internal reference CH₃Cl gas. Measured relative changes (showing negligible systematic errors) allowed calculation of the fractionation factor. From internal reference CH₃Cl gas, an overall reproducibility (1σ) for δ³⁷Cl(CH₃Cl) of 1.3‰, and a within day standard deviation ranging from 0.4 to 0.7‰, were determined for GC-MS measurements. Measured isotope ratios showed negligible effect of sample size across 2 orders of magnitude (0.5 to 10 ppmv) (Figs. S3 and S4).

Figure S1 and S2: Measurements of $\delta^{37}\text{Cl}(\text{CH}_3\text{Cl})$ values using GC-MS

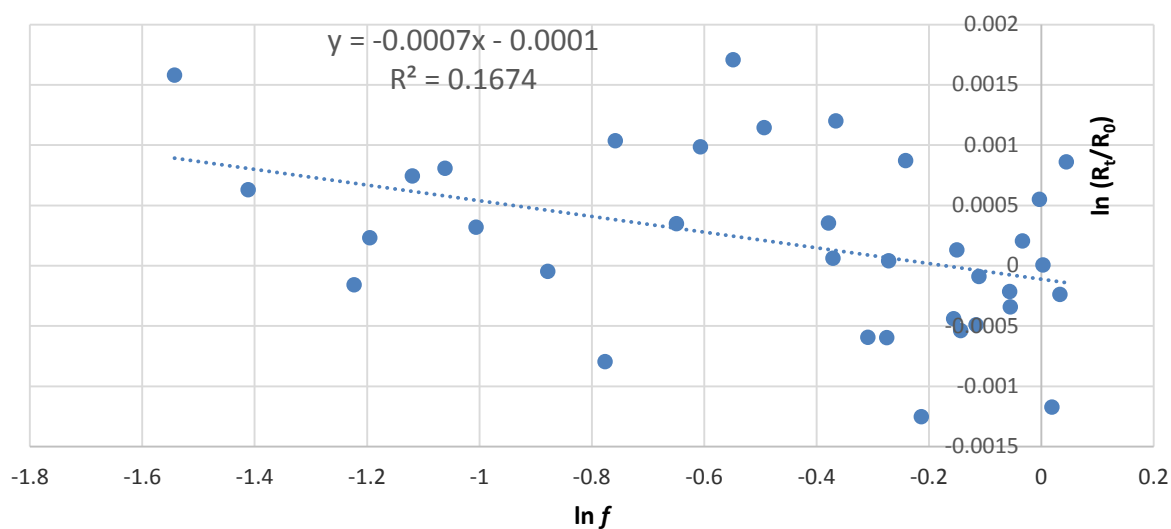


Figure S1: Rayleigh plot for gas phase reactions of CH_3Cl with $\cdot\text{OH}$ radicals derived from concentration measurements using GC-MS.

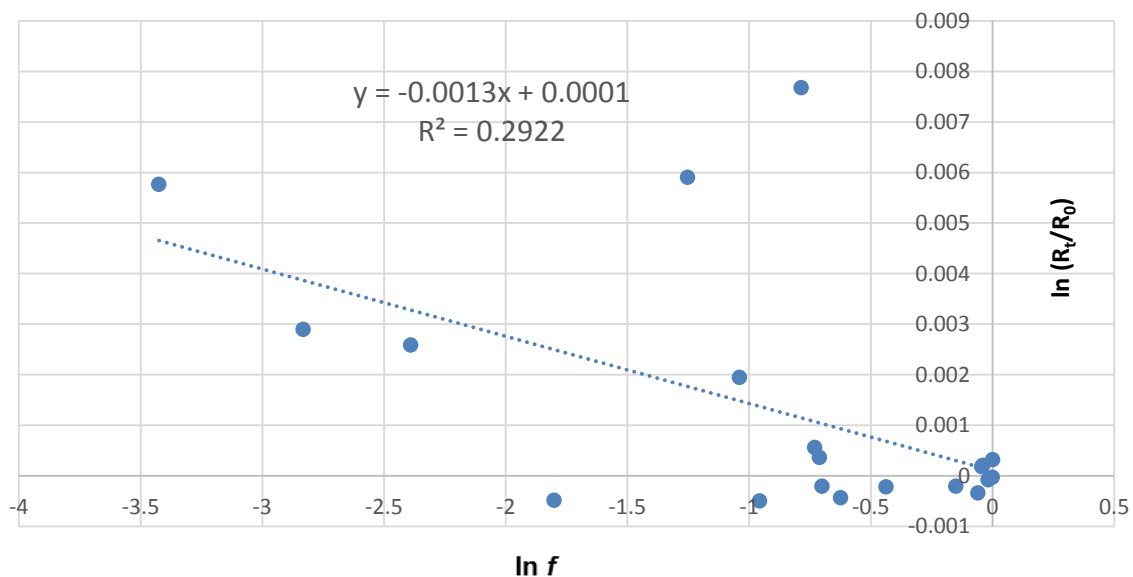


Figure S2: Rayleigh plot for gas phase reactions of CH_3Cl with $\cdot\text{Cl}$ radicals derived from concentration measurements using GC-MS.

Figure S3 and S4: GC-MS measurements and linearity of the $\delta^{37}\text{Cl}(\text{CH}_3\text{Cl})$ values

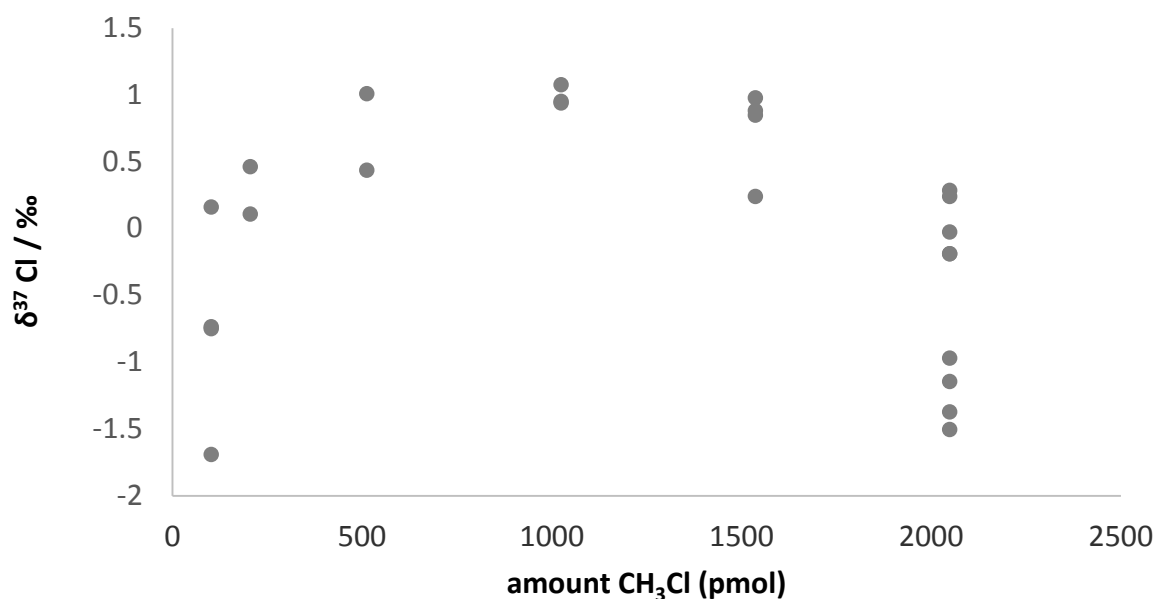


Figure S3: Plot of $\delta^{37}\text{Cl}$ versus amount of injected CH_3Cl standard. The overall standard deviation was 0.87 ‰. The data revealed no clear dependency of $\delta^{37}\text{Cl}$ values on the amount of CH_3Cl in the range from 100 to 2000 pmol.

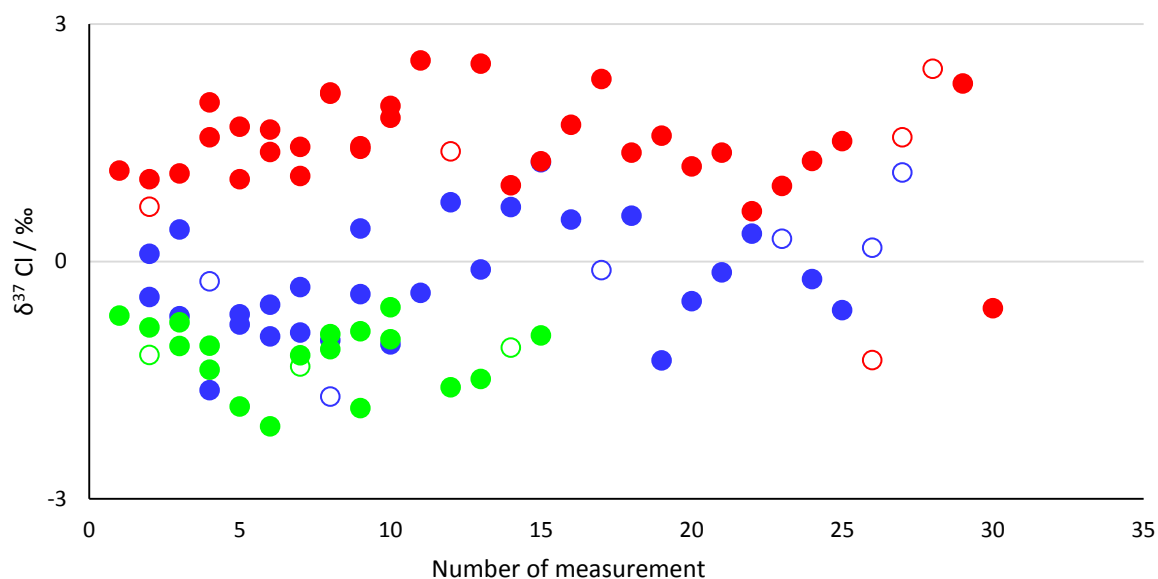


Figure S4: Variations in the $\delta^{37}\text{Cl}$ values of the measured standards during the degradation experiments in the smog chamber. Filled symbols denote a CH_3Cl amount of 2000 pmol and open symbols denote 200 pmol. The different colours indicate different experiments.

Method S2: Chloromethane purification line for CF-IRMS measurements

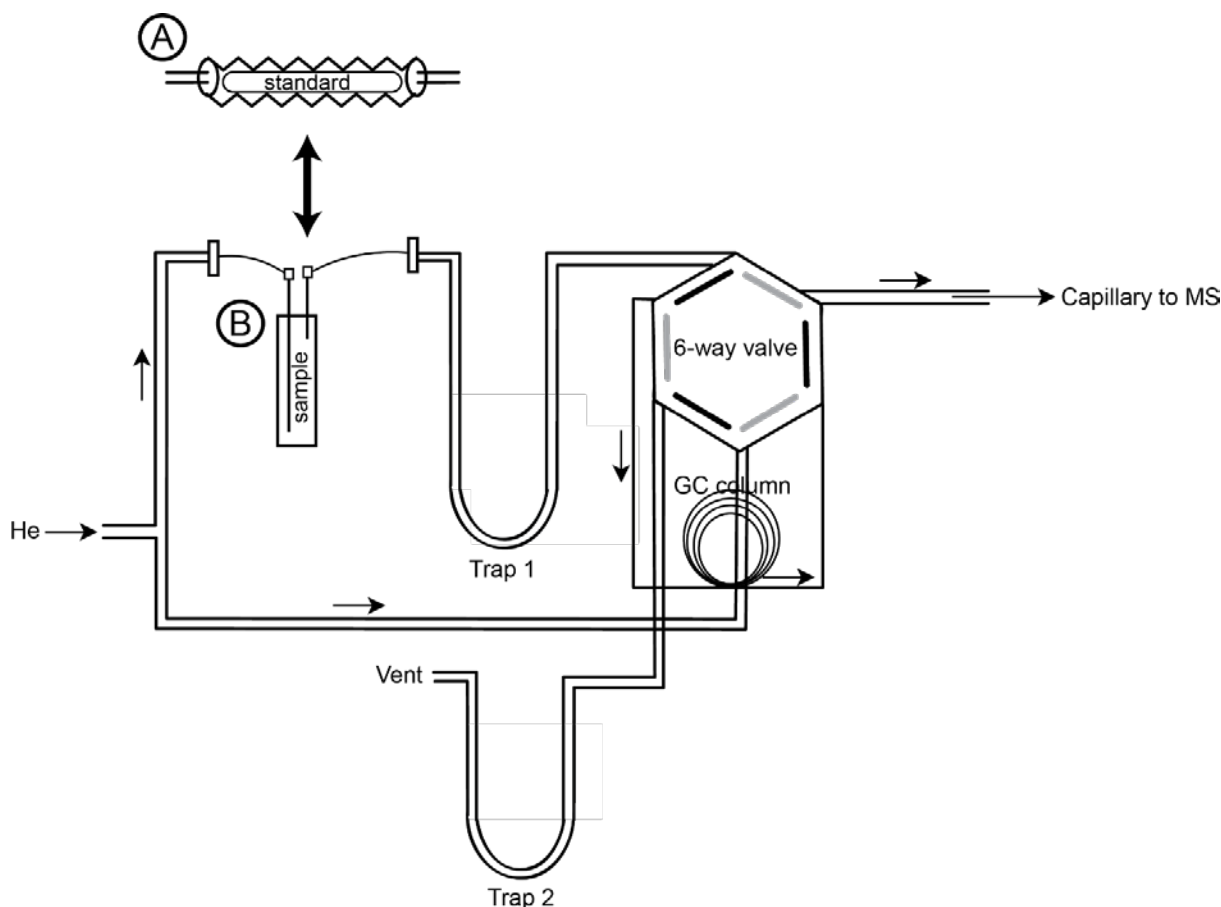


Figure S5: Schematic diagram showing the CH_3Cl purification line through which UHP helium (He) continuously flows. A) CH_3Cl (g) from seawater standards (sealed in a glass tube) are introduced into the tube cracker on the purification line. The tube is broken and the CH_3Cl is released to Trap 1 which is cooled in liquid nitrogen. After 3 minutes, the trap is warmed and the CH_3Cl is separated from excess CH_3I on the GC column, prior to introduction into the mass spectrometer (MS). Excess CH_3I is flushed from the GC column and frozen into Trap 2. B) For sample CH_3Cl (g) analyses, the tube cracker is removed from the line. Needles are attached to the line and introduced into the sample vial. The helium inlet needle penetrates to the bottom of the sample vial, whereas the vent needle penetrates a few mm below the septum. The sample CH_3Cl (g) is flushed from the vial with UHP helium and transferred to Trap 1 through the vent needle, where it is cryofocused with liquid nitrogen. After 3 minutes, the trap is warmed and the sample is introduced into the mass spectrometer. See³ for a more detailed description. Figure is modified from Barnes and Sharp (2006)³.

Method S3: Stable hydrogen and carbon isotope analysis using compound specific isotope ratio mass spectrometry

Stable hydrogen and carbon isotope ratios of CH₃Cl were measured by an in-house cryogenic pre-concentration unit coupled to a Hewlett Packard HP 6890 gas chromatograph (Agilent Technologies, Palo Alto, CA) and an isotope ratio mass spectrometer (IRMS) (Isoprime, Manchester, UK), as previously described^{4, 5}. For stable hydrogen isotope analysis, a ceramic tube reactor without chromium pellets at 1,450°C was used for high-temperature conversion. The CH₃Cl working standard was calibrated against IAEA standards NBS 22, LVSEC (carbon), VSMOW and SLAP (hydrogen) using TC/EA-IRMS (elemental analyzer-isotopic ratio mass spectrometer, IsoLab, Max Planck Institute for Biogeochemistry, Jena, Germany), yielding the following values: δ¹³C: -32.84 ± 0.06‰ (n=11, 1σ) and δ²H: -140.1 ± 1.0‰ (n=10, 1σ).

The conventional delta notation, expressing the isotopic composition of the sample relative to that of V-SMOW standard (Vienna Standard Mean Ocean Water) for hydrogen (δ²H_{V-SMOW}) and V-PDB standard (Vienna Pee Dee Belemnite) for carbon (δ¹³C_{V-PDB}) on per mil basis, was used.

Please note that the above described 1-point calibration of the δ²H(CH₃Cl) and δ¹³C(CH₃Cl) values might be affected by an additional error ("scale compression") and particularly might affect the uncertainties of the more positive δ¹³C(CH₃Cl) values. Unfortunately, CH₃Cl working standards with distinct isotopic signatures spanning the full range of measured δ¹³C(CH₃Cl) values (-32 ‰ to +91 ‰) are not currently available to eliminate or minimize such an error.

The mean precision based on replicate measurements (n = 6) of the CH₃Cl working standard was around 6 ‰ and 0.15 ‰ for δ²H(CH₃Cl) and δ¹³C(CH₃Cl) values, respectively. Samples

for measurements of $\delta^{13}\text{C}(\text{CH}_3\text{Cl})$ values were analyzed three times ($n = 3$), and the mean standard deviation (SD) of all measurements was 0.32 ‰. Samples for measurements of $\delta^2\text{H}(\text{CH}_3\text{Cl})$ were measured only one time.

The isotope fractionation ε was derived from the slope of the Rayleigh plot according to equation 1 which analogously was applied for $\delta^{13}\text{C}$ results:

$$\ln \frac{R}{R_0} = \ln \frac{(\delta^2 H_0 + \Delta \delta^2 H + 1)}{(\delta^2 H_0 + 1)} \cong (\alpha - 1) \cdot \ln f = \varepsilon \cdot \ln f \quad (1)$$

Figure S6 and S7: Chlorine isotope fractionation associated with microbial degradation of CH₃Cl

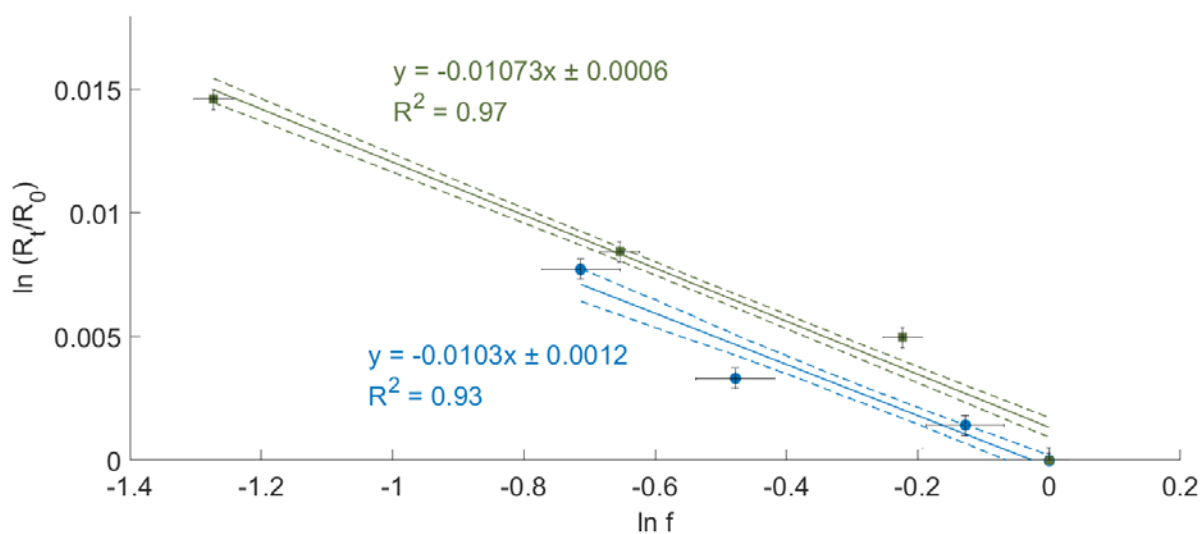


Figure S6: Rayleigh plots for degradation of CH₃Cl by *M. extorquens* CM4 during growth with CH₃Cl. Additional data for the two biological replicates where 3-4 time points were analysed for $\delta^{37}\text{Cl}(\text{CH}_3\text{Cl})$ values. Error bars were calculated by error propagation, including uncertainties in $\delta^{37}\text{Cl}(\text{CH}_3\text{Cl})$ values and the remaining fraction f . Dashed lines represent 95% confidence intervals of linear regressions (bold lines).

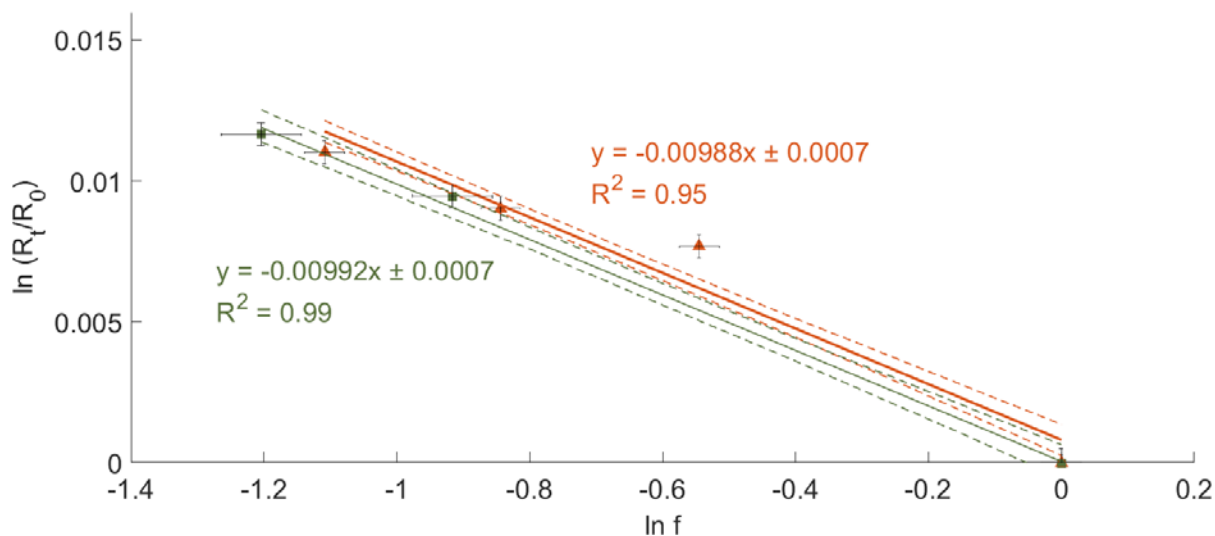


Figure S7: Rayleigh plots for degradation of CH₃Cl by *L. methylohalidivorans* MB2 during growth with CH₃Cl. Additional data for the two biological replicates where 3-4 time points were analysed for $\delta^{37}\text{Cl}(\text{CH}_3\text{Cl})$ values. Error bars were calculated by error propagation, including uncertainties in $\delta^{37}\text{Cl}(\text{CH}_3\text{Cl})$ values and the remaining fraction f . Dashed lines represent 95% confidence intervals of linear regressions (bold lines).

Figure S8 and S9: Carbon and hydrogen isotope fractionation associated with microbial degradation of CH₃Cl

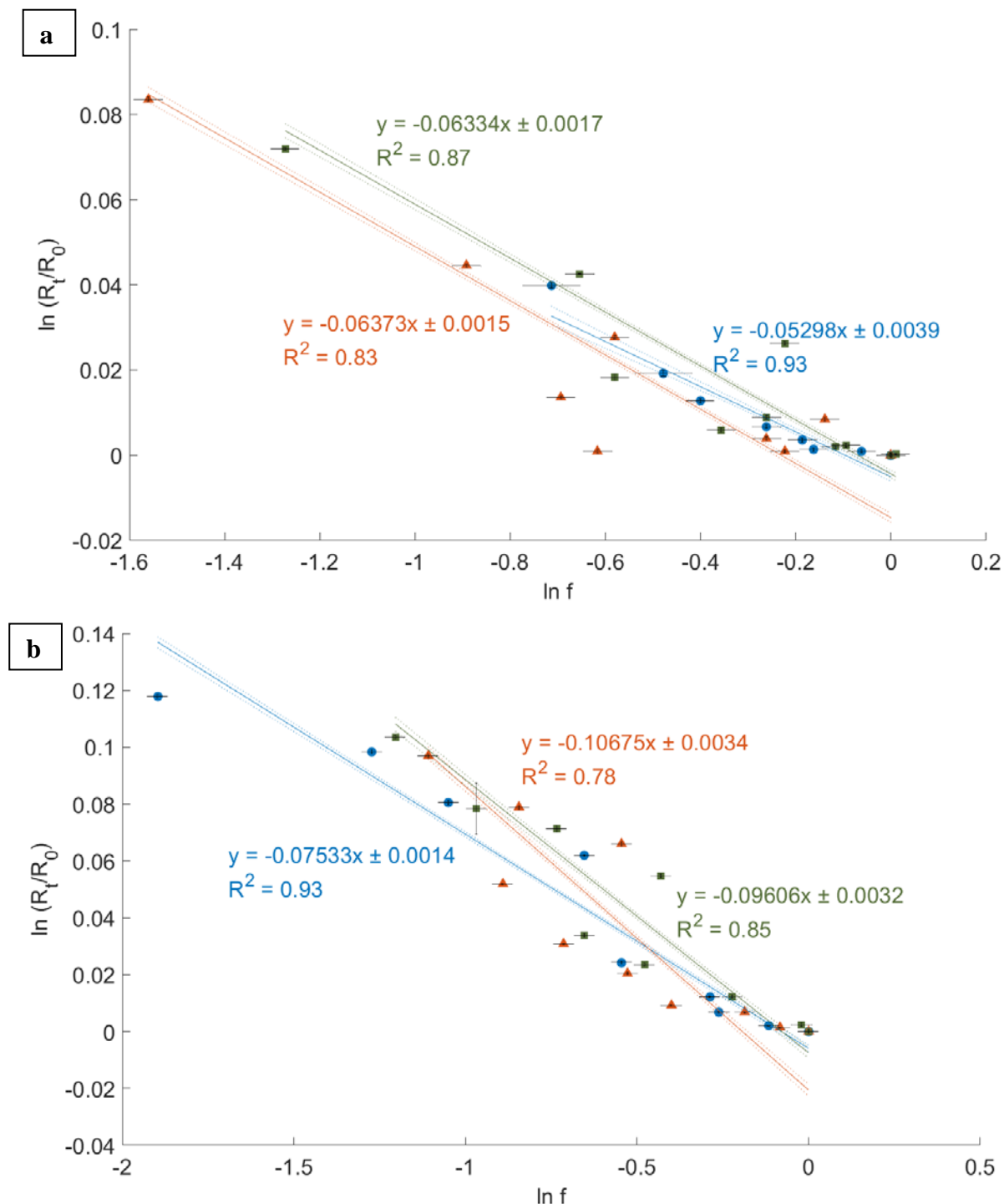


Figure S8: Carbon isotope fractionation during degradation of CH₃Cl by *M. extorquens* CM4 (a) and *L. methylohalidivorans* MB2 (b). Rayleigh plots from microbial CH₃Cl degradation experiments. Data from all three independent biological replicates are shown. Mean ϵ_C values obtained from the three biological replicates of *Methylobacterium extorquens* CM4 and *L. methylohalidivorans* MB2 values were $-59 \pm 6\%$ and $-92 \pm 16\%$, respectively.

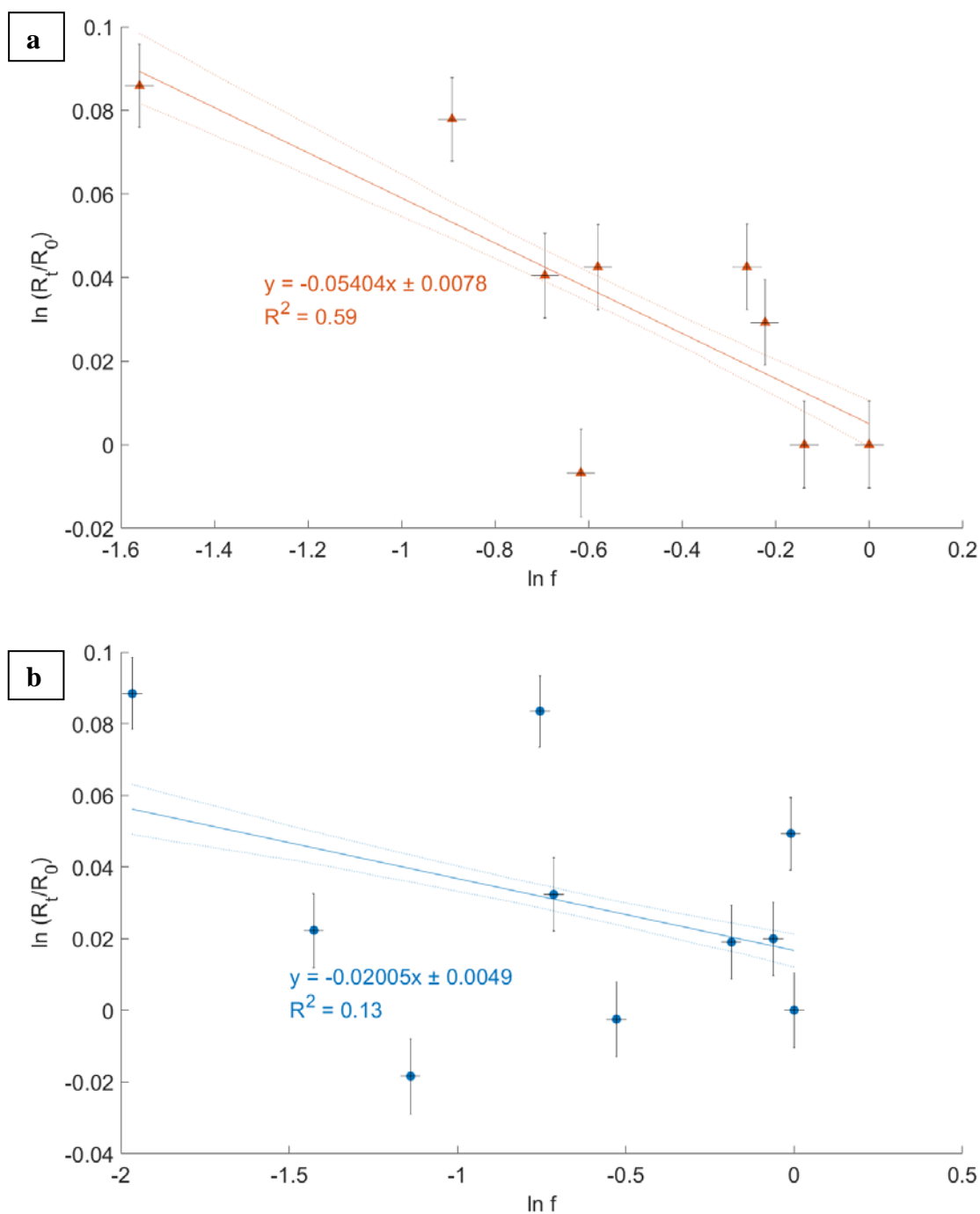


Figure S9: Hydrogen isotope fractionation during degradation of CH_3Cl by *M. extorquens* CM4 (a) and *L. methylohalidivorans* MB2 (b). Rayleigh plots from microbial CH_3Cl degradation experiments. Due to analytical difficulties during measurements of $\delta^2\text{H}(\text{CH}_3\text{Cl})$ values, only one series of biological replicates could be measured. Error bars were calculated by error propagation including uncertainties in $\delta^2\text{H}(\text{CH}_3\text{Cl})$ values and the remaining fraction f . Dashed lines represent 95% confidence intervals of the linear regressions (bold lines). Mean values of hydrogen fractionation (ϵ_{H} values) for CH_3Cl degradation by *M. extorquens* CM4 and *L. methylohalidivorans* MB2 were determined as $-54 \pm 8\%$ and $-20 \pm 5\%$, respectively.

References

1. Bahlmann, E.; Keppler, F.; Wittmer, J.; Greule, M.; Schöler, H. F.; Seifert, R.; Zetzsch, C., Evidence for a major missing source in the global chloromethane budget from stable carbon isotopes. *Atmos. Chem. Phys.* **2019**, *19*, (3), 1703-1719.
2. Keppler, F.; Bahlmann, E.; Greule, M.; Schöler, H. F.; Wittmer, J.; Zetzsch, C., Mass spectrometric measurement of hydrogen isotope fractionation for the reactions of chloromethane with OH and Cl. *Atmos. Chem. Phys.* **2018**, *18*, (9), 6625-6635.
3. Barnes, J. D.; Sharp, Z. D., Achlorine isotope study of DSDP/ODP serpentinized ultramafic rocks: Insights into the serpentinization process. *Chem. Geol.* **2006**, *228*, (4), 246-265.
4. Nadalig, T.; Greule, M.; Bringel, F.; Keppler, F.; Vuilleumier, S., Probing the diversity of chloromethane-degrading bacteria by comparative genomics and isotopic fractionation. *Front. Terr. Microbiol.* **2014**, *5*, 523, doi:10.3389/fmicb.2014.00523.
5. Jaeger, N.; Besaury, L.; Kröber, E.; Delort, A.-M.; Greule, M.; Lenhart, K.; Nadalig, T.; Vuilleumier, S.; Amato, P.; Kolb, S.; Bringel, F.; Keppler, F., Chloromethane Degradation in Soils: A Combined Microbial and Two-Dimensional Stable Isotope Approach. *J. Environ. Qual.* **2018**, *47*, (2), 254-262.